


GPRC5A facilitates cell proliferation through cell cycle regulation and correlates with bone metastasis in prostate cancer

Yuichiro Sawada^{1,2,3}, Tadahiko Kikugawa¹, Hiroyuki Iio^{1,2,3}, Iori Sakakibara⁴, Shuhei Yoshida², Aoi Ikedo³, Yuta Yanagihara^{2,3,5}, Noritaka Saeki^{3,5}, Balázs Györfy^{6,7}, Takeshi Kishida⁸, Yoichiro Okubo⁹, Yoshiyasu Nakamura¹⁰, Yohei Miyagi¹⁰, Takashi Saika¹ and Yuuki Imai¹⁰ 

¹Department of Urology, Ehime University Graduate School of Medicine, Toon, Japan

²Department of Pathophysiology, Ehime University Graduate School of Medicine, Toon, Japan

³Division of Integrative Pathophysiology, Proteo-Science Center, Ehime University, Toon, Japan

⁴Research Center for Advanced Science and Technology, The University of Tokyo, Tokyo, Japan

⁵Division of Laboratory Animal Research, Advanced Research Support Center, Ehime University, Toon, Japan

⁶MTA TTK Lendület Cancer Biomarker Research Group, Institute of Enzymology, Hungarian Academy of Sciences, Budapest, Hungary

⁷Semmelweis University 2nd Dept. of Pediatrics, Budapest, Hungary

⁸Department of Urology, Kanagawa Cancer Center, Yokohama, Japan

⁹Department of Pathology, Kanagawa Cancer Center, Yokohama, Japan

¹⁰Molecular Pathology and Genetics Division, Kanagawa Cancer Center Research Institute, Yokohama, Japan

The prognosis of patients with progressive prostate cancers that are hormone refractory and/or have bone metastasis is poor. Multiple therapeutic targets to improve prostate cancer patient survival have been investigated, including orphan GPCRs. In our study, we identified G Protein-Coupled Receptor Class C Group 5 Member A (GPRC5A) as a candidate therapeutic molecule using integrative gene expression analyses of registered data sets for prostate cancer cell lines. Kaplan–Meier analysis of TCGA data sets revealed that patients who have high GPRC5A expression had significantly shorter overall survival. PC3 prostate cancer cells with CRISPR/Cas9-mediated GPRC5A knockout exhibited significantly reduced cell proliferation both *in vitro* and *in vivo*. RNA-seq revealed that GPRC5A KO PC3 cells had dysregulated expression of cell cycle-related genes, leading to cell cycle arrest at the G2/M phase. Furthermore, the registered gene expression profile data set showed that the expression level of GPRC5A in original lesions of prostate cancer patients with bone metastasis was higher than that without bone metastasis. In fact, GPRC5A KO PC3 cells failed to establish bone metastasis in xenograft mice models. In addition, our clinical study revealed that GPRC5A expression levels in prostate cancer patient samples were significantly correlated with bone metastasis as well as the patient's Gleason score (GS). Combined assessment with the immunoreactivity of GPRC5A and GS displayed higher specificity for predicting the occurrence of bone metastasis. Together, our findings indicate that GPRC5A can be a possible therapeutic target and prognostic marker molecule for progressive prostate cancer.

Author contributions: Study design and experimental design: Sawada Y, Imai Y. Experimental and data analysis: Sawada Y, Iio H, Sakakibara S, Yanagihara Y, Yoshida S, Saeki N. Statistical analyses: Ikedo A with Sawada Y. Kaplan–Meier plot analysis: BG. Clinical study: Kikugawa T, Nakamura Y, Okubo Y, Miyagi Y. Experimental design and data interpretation: Kishida T, Saika T. Manuscript writing, with input from the other authors: Sawada Y, Imai Y.

Additional Supporting Information may be found in the online version of this article.

Key words: GPCR, prostate cancer, bone metastasis, GPRC5A

Abbreviations: ADT: androgen deprivation therapy; AR: androgen receptor; ARV7: androgen receptor splice variant-7; cAMP: cyclic adenosine monophosphate; CDK: cyclin-dependent kinases; CREB: cAMP response element binding protein; CRPC: castration-resistant prostate cancer; DAVID: Database for Annotation, Visualization and Integrated Discovery; ER: endoplasmic reticulum; GEO: Gene Expression Omnibus; GPCR: G protein-coupled receptor; GPRC5A: G protein-coupled receptor class C group 5 member A; GS: Gleason score; GSEA: Gene Set Enrichment Analysis; HSD3B1: hydroxy-delta-5-steroid dehydrogenase, 3 beta- and steroid delta-isomerase 1; PKA: protein kinase A; PSA: prostate-specific antigen; RAIG1: retinoic acid-induced gene 1; RMA: robust multiarray average; SRE: skeletal-related event; TCGA: The Cancer Genome Atlas

Conflict of interest: The authors declare no potential conflicts of interest.

Grant sponsor: Japan Society for the Promotion of Science; **Grant number:** KAKENHI Grants JP18K09168; **Grant sponsor:** Takeda Science Foundation

DOI: 10.1002/ijc.32554

History: Received 24 Jan 2019; Accepted 24 Jun 2019; Online 5 Jul 2019

Correspondence to: Yuuki Imai MD, PhD, Shitsukawa, Toon, Ehime 791-0295, Japan, Tel.: +81-89-960-5925, Fax: +81-89-960-5953, E-mail: y-imai@m.ehime-u.ac.jp

What's new?

Although androgen deprivation is effective in most prostate cancer patients, cellular pathways outside androgen receptor signaling are being explored to treat castration-resistant cancer forms. Here the authors focus on GPCR5A, an orphan G protein-coupled receptor, they find is overexpressed in prostate cancer cell lines. Knockout of GPCR5A decreased proliferation of a prostate cancer cell line and prevented bone metastasis in a xenograft model. In patients, GPCR5A expression correlated with shorter overall survival and bone metastasis, underscoring its clinical potential as a therapeutic or prognostic target.

Introduction

The rate of prostate cancer is increasing worldwide, particularly among older populations. Prostate cancer is a carcinoma that is highly curable with early diagnosis and early treatment. However, patients with progressive prostate cancer often have decreased quality of life due to visceral organ and bone metastasis, as well as worsened prognosis and increased pain and frequency of skeletal-related events.¹ Androgen deprivation therapy (ADT) is the most prominent treatment strategy for locally invasive or advanced prostate cancer. Although ADT is extremely effective for more than 90% of prostate cancer patients, some cases can become refractory to ADT, whereas for other cases, several years after diagnosis the disease shifts to castration-resistant prostate cancer (CRPC).²

Current proposed mechanisms for progression to CRPC involve amplification of the androgen receptor (AR), mutations in the AR gene, variant AR expression levels, activation of transcriptional coactivators of AR, phosphorylation of ligand-independent AR and/or activation of proliferative signaling in the absence AR.³ Various medications such as chemotherapy using docetaxel and cabazitaxel for CRPC, and novel antiandrogen drugs such as abiraterone and enzalutamide are commonly used to treat progressive prostate cancers, although there is currently no established consensus therapy.⁴ In addition, there are significant differences in the efficacy of enzalutamide therapy between patients harboring variants of hydroxy-delta-5-steroid dehydrogenase, 3 beta- and steroid delta-isomerase 1 (HSD3B1) and AR such as androgen receptor splice variant-7 (ARV7) and those who do not.^{5,6} Therefore, investigations of novel therapeutic target molecules outside of AR signaling pathways are needed to develop new therapeutic strategies for CRPC and progressive prostate cancer. Day *et al.*⁷ reported that epithelial cell growth factor (EGF) and its receptor (EGF-R) are expressed in prostate cancer tissue and that expression levels of these proteins correlate with survival rate. Furthermore, other growth factors such as vascular endothelial growth factor (VEGF) and insulin-like growth factor (IGF) are related to prostate cancer progression.⁸ Malinowska *et al.*⁹ reported that various cytokines are important for the progression of prostate cancer. Many of these growth factors and cytokines bind receptors on the plasma membrane; most of these receptors can be categorized as G protein-coupled receptors (GPCRs). Such GPCRs are possible therapeutic targets not only for prostate cancer but also many other types of carcinomas.¹⁰

Among the GPCRs, orphan GPCRs have high potential as therapeutic targets.¹¹ Some orphan GPCRs, such as GPCR6A and GPR160, are involved in prostate cancer cell proliferation

and disease progression.^{12,13} However, the significance of other orphan GPCRs in prostate cancer is elusive. In our study, we sought to identify orphan GPCRs that could serve as novel therapeutic target molecules for progressive prostate cancer.

The origin, androgen sensitivity and prostate-specific antigen (PSA) expression levels vary among representative prostate cancer cell lines such as PC3, DU145 and LNCaP.¹⁴ For our study, we analyzed registered and publicly available gene expression profiling data for prostate cancer cell lines with a focus on androgen sensitivity and bone metastatic capacity due to the association of these features with prognosis. We found that G protein-coupled receptor class C group 5 member A (GPCR5A) had the highest differential expression among orphan GPCRs in progressive prostate cancer cells. GPCR5A is classified into GPCR class C group 5 member A that can be induced by retinoic acid stimulation and are important for embryonic development, differentiation, tumorigenesis and maintenance of epithelial homeostasis.^{15,16} GPCR5A participates in lung tissue homeostasis, and is expressed in pulmonary epithelial cells.¹⁶ Several reports showed that GPCR5A expression is increased in pancreatic cancer, colon cancer, breast cancer and myelodysplastic syndrome.^{17–20} On the other hand, GPCR5A has a dual behavior as a tumor suppressor. GPCR5A expression is suppressed in lung cancer and works as a negative modulator of EGFR signaling.^{21–23} Zhou *et al.* reported that the high expression level of GPCR5A in prostate cancer.²⁰ However, there is no information concerning GPCR5A function in prostate cancer. Results from *in vitro*, *in vivo* and clinical studies support a key role of GPCR5A in prostate cancer progressiveness and bone metastasis.

Materials and Methods**Gene expression microarray analysis**

Gene expression analysis of orphan GPCRs was performed using microarray data sets for untreated prostate cancer cell lines PC3, DU145 and LNCaP registered in the GEO (<http://www.ncbi.nlm.nih.gov/geo/>; Supporting Information Table S1). The raw data were normalized by robust multiarray average (RMA)²⁴ using R software provided by The Comprehensive R Archive Network (<https://cran.r-project.org/>). Raw data for the clinical prostate cancer sample microarray²⁵ were retrieved and analyzed using OncoPrint (<https://www.oncoPrint.org/>; Supporting Information Table S2). GPCR5A expression in nonmetastatic cases and bone metastasis of CRPC cases was analyzed by GEO2R.

TCGA RNA sequence analysis

Gene expression analysis of cell cycle-related genes in Human lung cancer and prostate cancer was performed using The

cBioPortal for Cancer Genomics (<http://cbioportal.org>). Lung Adenocarcinoma (The Cancer Genome Atlas [TCGA], Provisional, 586 samples) and Prostate Adenocarcinoma (TCGA, Provisional, 499 samples) were selected as data set of human lung cancer and prostate cancer.

Cell culture

PC3-Luc cells were purchased from the JCRB Cell Bank and cultured in Ham's F-12K medium (Wako, Japan) supplemented with 7% fetal bovine serum and antibiotic-antimycotic (Thermo Fisher Scientific, Waltham, MA). DU145 and LNCaP cell lines were cultured in RPMI-1640 medium (Wako, Japan) supplemented with 10% fetal bovine serum and antibiotic-antimycotic. Cells were cultured at 37°C in 5% CO₂ humidified air.

GPRC5A knockout by CRISPR/Cas9

GPRC5A was knocked out using the Guide-it™ CRISPR/Cas9 System (Clontech Laboratories, Inc., Mountain View, CA). The guide RNA (gRNA) sequence and primers for sequence confirmation were designed using the online program CHOP-CHOP (<http://chopchop.cbu.uib.no/>).^{26,27} Vectors incorporating the guide RNA were transfected into PC3-Luc cells and DU145 cells with ScreenFect A (Wako, Japan) according to the manufacturer's protocol and analyzed using the FACSARIA™ Special Order System (Becton Dickinson and Company, Franklin Lakes, NJ). ZsGreen was selected as a reporter for transfection into single cells.

Real-time RT-PCR

Total RNA extracted using ISOGEN (Nippongene, Japan) and an RNeasy spin column kit (Qiagen, Germantown, MD) was treated with DNase I (Qiagen). Subsequently, complementary DNA was synthesized from 500 ng total RNA using PrimeScript RT Master Mix (Takara Bio Inc., Kusatsu, Japan). Real-time RT-PCR was carried out using Thermal Cycler Dice (Takara Bio Inc.) and SYBR Premix Ex Taq II (Takara Bio Inc.) according to the manufacturer's protocol. Gene expression levels were normalized relative to expression levels of the housekeeping gene RPLP0. All primer sequences are listed in the Supporting Information Table S3.

Cell growth assay

Cells were seeded at 1×10^4 cells/well in a 96-well plate and measured the MTT cell number measurement kit (Nacalai Tesque, Japan) and the 5-Bromo-2'-deoxyuridine (BrdU) incorporation assay (Roche, Germany) according to the manufacturer's protocol.

Cell migration assay

Cells were seeded in six-well plates at a density equivalent to 100% confluence. Growth was suppressed by exposure to starvation conditions for 24 hr in a medium containing 1% FBS (Ham's F-12K medium, Wako, Japan), and each well was scratched using a 200 μ l pipette tip. Thereafter, the medium was exchanged with serum-free medium (Ham's F-12K medium,

Wako, Japan) and cultured for 24 hr before measurement of the number of migrating cells per equivalent unit area.

Cell cycle assay

Cells were seeded at 1×10^5 cells/well in 6-well plates. At 48 hr after seeding, a BD Cycletest™ Plus DNA Kit (BD Biosciences, USA) was used according to the manufacturer's protocol to purify the sample and the cell cycle status was evaluated by flow cytometry (Gallios flow cytometer, Beckman Coulter, Brea, CA).

Lentiviral infection and plasmid vectors

Human GPRC5A cDNA was cloned into the lentiviral backbone CSII-CMV-MCS-IRES2-Bsd (RDB04385, Riken, Japan). The plasmid was transfected with pCAG-HIVgp (RDB04394, Riken, Japan) and pCMV-VSV-G-RSV-Rev (RDB04393, Riken, Japan) into the HEK293T Packaging Cell Line using ScreenFect A (cat. no. 299-73203, Wako, Japan) according to the manufacturer's instructions. Lentiviral infection was accomplished at 37°C 24 hr using HEK293T supernatant supplemented and the infected cells were selected by blasticidin treatment.

Animals

BALB/cAJcl-nu nude male mice (CLEA Japan, Inc., Tokyo, Japan) were housed in a specific pathogen-free facility under climate-controlled conditions at room temperature ($22 \pm 2^\circ\text{C}$) with 50% humidity and a 12-hr light/dark cycle. Mice were provided with water and standard diet (MF, Oriental Yeast Co., Ltd., Tokyo, Japan) *ad libitum*. Animal experiments were approved by the Animal Experiment Committee of Ehime University (Approval No. 37A5-16) and were performed in accordance with Ehime University Guidelines for Animal Experiments.

Human prostate cancer cell xenografts

For subcutaneous implantation, 1×10^6 of cells were suspended in Matrigel Basement Membrane HC (Corning, Corning, NY). After anesthesia with isoflurane, cell fluid was injected into the subcutaneous space on the backs of 5-week-old male nude mice using a 26 G needle. Five weeks after inoculation, the mice were evaluated by *in vivo* imaging and then euthanized, and the tumors were removed and fixed with 4% paraformaldehyde phosphate buffer solution (Wako) and used for histological examination. For tibial intramedullary transplantation, 1×10^4 of cells were suspended in 10 μ l sterile PBS. Under anesthesia with isoflurane, a hole was drilled in the cortical bone of the tibial tuberosity using a 27 G needle and cells were transplanted using a 29 G needle. Beginning 3 weeks after transplantation, tumor cell engraftment and proliferation were evaluated weekly by *in vivo* imaging. The animals were euthanized 6 weeks after transplantation and tibiae were collected for bone morphometry, bone density measurement and histological analysis.

In vivo imaging

Mice were placed on an AEQUORIA-2D/8600 (Hamamatsu Photonics K. K., Shizuoka, Japan) platform under isoflurane

anesthesia and signals were detected 5 min after intraperitoneal injection of 100 μ l of 40 mg/ml D-luciferin (Wako, Japan) in PBS. The luminescence images were quantitatively analyzed as integrated density in the same area using ImageJ.

Radiological examinations

Tibial bone mineral density (BMD) was assessed by dual-energy X-ray absorption measurements using a bone mineral analyzer (DCS-600 EX Aloka, Japan). Micro computerized tomography scan was performed using μ CT35 system (SCANCO Medical, Switzerland) as previously described.²⁸

Histological evaluation

Subcutaneously implanted samples were embedded in paraffin. Tibial samples were embedded in paraffin after decalcification with Morse solution. Paraffin sections were then cut into 10 μ m-thick slices with a microtome (RM 2255, Leica Biosystems, Wetzlar, Germany). Sections were deparaffinized before HE and TRAP staining using a TRAP/ALP Stain kit (Wako, Japan) according to the manufacturer's protocol. For fluorescent immunostaining of the subcutaneously transplanted samples, sections were treated with citrate buffer (pH 6.0) and microwaved for antigen retrieval. After washing with PBS, blocking was carried out for 30 min at room temperature with goat serum (Wako, Japan) diluted 1:50 with PBS. Antiluciferase antibody (catalog number PM016, MBL, Japan) and anti-Ki67 antibody (catalog number 14-5698-82, Invitrogen) were diluted 1:200 with antibody diluent (Dako, Japan) and incubated at 4°C for overnight. After washing with PBS, a secondary antibody reaction was performed.

Immunohistochemical analyses of human prostate cancer specimens

Immunohistochemical analyses (IHC) of GPRC5A expression were conducted on needle biopsy specimens in the archives of the Kanagawa Cancer Center Department of Pathology. For these samples, 12 prostatic needle cores were obtained transperineally from the patient and a Gleason score (GS) was assigned for each core that contained prostatic adenocarcinoma tissues according to the 2005 International Society of Urological Pathology (ISUP) consensus conference.²⁹ The highest GS was designated as the patient GS and the biopsy specimen from each patient that had the highest GS was selected for IHC. In total, specimens from 255 samples collected between 2011 and 2015 from prostate cancer patients having GS 7 and higher and who had not undergone prior treatment were evaluated for GPRC5A expression (115, GS 7: 69, GS 8: 73, GS9: 3, GS 10). All patients were evaluated for bone metastasis around the time of needle biopsy by computerized tomography (CT) and bone scintigraphy with ^{99m}Tc-tetechium-methylene diphosphonate (MDP). The research ethics committees of Kanagawa Cancer Center and Ehime University approved our study under protocol no. 2018 epi-11 and 1806001, respectively. Thin (4 μ m-thick) sections were prepared from formalin-fixed and paraffin-embedded needle

biopsy specimens and subjected to IHC. Briefly, the antigen was retrieved by incubating the specimen in citrate buffer (pH 6.0) in a steamer for 15 min. Endogenous peroxidase activity and nonspecific antibody binding were blocked with 3% hydrogen peroxide and a blocking reagent (Biocare Medical, Pacheco, CA), respectively. A rabbit monoclonal antibody raised against human retinoic acid-induced gene 1 (RAIG1; clone D4S7D, Cell Signaling Technology, Danvers, MA; RAIG1 is an alternate name for GPRC5A) was applied at 1:800 dilution, and immunoreactivity was visualized using the peroxidase-labeled amino acid polymer method in the MAX-PO Histofine simple stain kit (Nichirei Co., Tokyo, Japan) according to the manufacturer's instructions. IHC results were read independently by three investigators and classified according to the percentage of staining area. Low and High immunoreactivity groups were defined as GPRC5A-positive sites occupying <10% or >10% of the cancer area, respectively. Evaluations were concordant in 95% of the readings; differences were resolved by consensus after joint review.

RNA sequence and data analyses

Total RNA was collected from Control PC3-Luc and the two GPRC5A KO cell lines as described above and RNA-seq was performed as previously described.²⁸ Mapping to human genome data hg38 was performed using Tophat, and the expression analysis tool Cufflinks was used to normalize each sample before determining the differences in expression between Control ($n = 3$) and GPRC5A KO 1 and KO 2 ($n = 6$) by tmm using R. Raw and processed data were registered to the GEO (GSE121319). Gene Ontology analyses were performed using Database for Annotation, Visualization and Integrated Discovery (DAVID) Bioinformatics Resources 6.7³⁰ and Gene Set Enrichment Analysis (GSEA).³¹

Survival analysis

The RNA-seq data for prostate cancer patients was obtained from the TCGA repository (<https://cancergenome.nih.gov/>), with overall survival information available for 421 patients. The raw data was DEseq-normalized and the RNA-seq ID 9052 was used for GPRC5A. Only patients who had adenocarcinoma and a GS of at least 8 were included in the analysis ($n = 183$). Correlation to overall survival was tested by Cox proportional hazards regression. The upper quartile of expression was used to split the patients into two cohorts. Analyses including Kaplan–Meier survival plots, hazard ratios with 95% confidence interval and log-rank p -values were calculated and plotted in R using Bioconductor packages.

Statistical analysis

All graphs represent mean \pm SD. Significant differences between mean values were determined by two-tailed Student's t -test or Mann Whitney U test for comparison between two groups, or one-way ANOVA and *post hoc* Student Newman–Keuls test for comparison between three or more groups using Microsoft Excel or EZR version 1.35,³² or GraphPad Prism

7 or SPSS version 25. The area under ROC curve (AUC) was calculated to assess overall diagnostic accuracy and to identify optimal cutoffs for risk factors for bone metastasis. AUC was assessed using standard criteria.³³ The optimal cutoffs were determined and the sensitivity, specificity, positive and negative predictive values as well as diagnostic accuracy for bone metastasis were calculated.

Results

GPRC5A is highly expressed in androgen-insensitive prostate cancer cell lines and correlated with poor prognosis of prostate cancer patients

Representative prostate cancer cell lines, including LNCaP as an androgen-sensitive prostate cancer cell line as well as PC3 and DU145 as androgen-insensitive cell lines with high malignancy potential were analyzed. Microarray data sets for these cell lines were obtained from the NCBI Gene Expression Omnibus (GEO; PC3: $n = 9$, DU145: $n = 6$, LNCaP: $n = 33$ array data sets). A heatmap highlighted the differential expression levels of orphan GPCR genes in PC3 and DU145 compared to LNCaP (Supporting Information Fig. S1). In particular, among orphan GPCR class C family members, GPRC5A expression levels were significantly higher in both PC3 and DU145 cells relative to LNCaP, with increases of more than fivefold in microarray signals (Fig. 1a). RT-qPCR assays to quantitate GPRC5A expression levels in these three cell lines confirmed that the expression level of GPRC5A in PC3 and DU145 cells was indeed significantly higher than that of LNCaP (Fig. 1b). These results indicate that high expression levels of GPRC5A might be related to prostate cancer progression. To test this possibility, the correlation between GPRC5A expression intensity and human prostate cancer case outcomes was analyzed *in silico* using RNA-seq data from The Cancer Genome Atlas (TCGA) project. Patients with high GPRC5A expression had significantly shorter overall survival (Fig. 1c), suggesting that high expression levels of GPRC5A could correlate with progressive prostate cancer.

Involvement of GPRC5A in prostate cancer cell proliferation both *in vitro* and *in vivo*

To ascertain the role of GPRC5A in prostate cancer, GPRC5A knockout (KO) in PC3-Luc and DU145 cells was established using CRISPR/Cas9 genome editing (Supporting Information Figs. S2a and S2b). Cell proliferation and viability determined by BrdU incorporation (Fig. 1d) and MTT assay (Fig. 1e and Supporting Information Fig. S2c), respectively, were significantly decreased in GPRC5A KO cells, although apoptosis rates were not (Supporting Information Fig. S3a). In addition, GPRC5A KO cells had significantly reduced migration ability (Fig. 1f) that could be related to decreased cell proliferation. On the other hand, the invasion activity (Supporting Information Fig. S3b) and adhesion capacity (Supporting Information Fig. S3c) of GPRC5A KO cells were slightly increased in GPRC5A KO cells relative to cells that expressed GPRC5A. These results indicate that GPRC5A is mainly involved in prostate cancer cell proliferation.

Next, to investigate the pathophysiological role of GPRC5A in prostate cancer progression, we analyzed tumor growth of GPRC5A KO PC3-Luc cells using an *in vivo* subcutaneous xenograft mice model. *In vivo* bioluminescence images acquired 4 weeks after inoculation showed substantially lower luciferase signals (Fig. 2a) and significantly reduced integrated density (Fig. 2b) in GPRC5A KO groups. The size and weight of excised tumors were remarkably decreased in GPRC5A KO groups relative to those from mice implanted with control cells (Figs. 2c and 2d). Hematoxylin and eosin (HE) staining of the excised tumors showed that tumor cells were homogeneously located throughout the tumors in the control group, whereas tumor cells were sparsely located between extracellular matrices in the GPRC5A KO groups (Fig. 2e). In addition, immunohistochemistry against luciferase and Ki67 revealed that the number of cells that were double positive for luciferase and Ki67 staining among luciferase positive cells in tumors was significantly lower in the GPRC5A KO group relative to the control (Figs. 2f and 2g). These data suggest that GPRC5A positively controls prostate cancer cell proliferation *in vitro* and *in vivo*.

GPRC5A regulates the expression of cell cycle-related genes in prostate cancer cells

To elucidate the detailed molecular mechanism underlying GPRC5A-mediated prostate cancer cell proliferation, we performed RNA sequencing (RNA-seq) on control PC3 cells and GPRC5A KO PC3 cells. A volcano plot indicated that 511 and 443 genes were significantly upregulated and downregulated, respectively, in GPRC5A KO cells (Fig. 3a). For these differentially expressed genes, we performed gene ontology (GO) analyses using the DAVID and GSEA to examine the downstream effects of GPRC5A expression. Genes involved in cell cycle, mitosis and cell division were significantly enriched in biological processes in GPRC5A KO cells by DAVID analysis (Fig. 3b) and 16 gene sets were enriched with NES > 1.5. Among these genes, GSEA analysis showed that eight gene sets were directly related to cell cycle (Supporting Information Fig. S4a). Gene sets for cell cycle process (Fig. 3c), M phase and mitosis (Supporting Information Fig. S4b) showed a strong correlation with GPRC5A KO. On the other hand, no association with cell proliferation was found in analyses of genes that showed GPRC5A-dependent downregulation (Supporting Information Fig. S4c). These results indicate that the reduced cell proliferation phenotypes seen for GPRC5A KO PC3 cells were induced by disrupted expression of cell cycle-related genes. To test this possibility, the expression levels of representative cell cycle-related genes including cyclins (CCNs) and cyclin-dependent kinases (CDKs) present during each cell cycle phase were examined. RT-qPCR revealed that the expression of G2 phase genes such as *CCNA2* and *CDK1* and M phase genes such as *CCNB1* and *CCNB2* was significantly elevated in the presence of GPRC5A KO in both PC3 and DU145 cell (Fig. 3d and Supporting Information Fig. S5a). On the other hand, expression of the G1 phase gene *CCND1* was decreased by GPRC5A KO in PC3, not in DU145 (Fig. 3d and Supporting Information Fig. S5a).

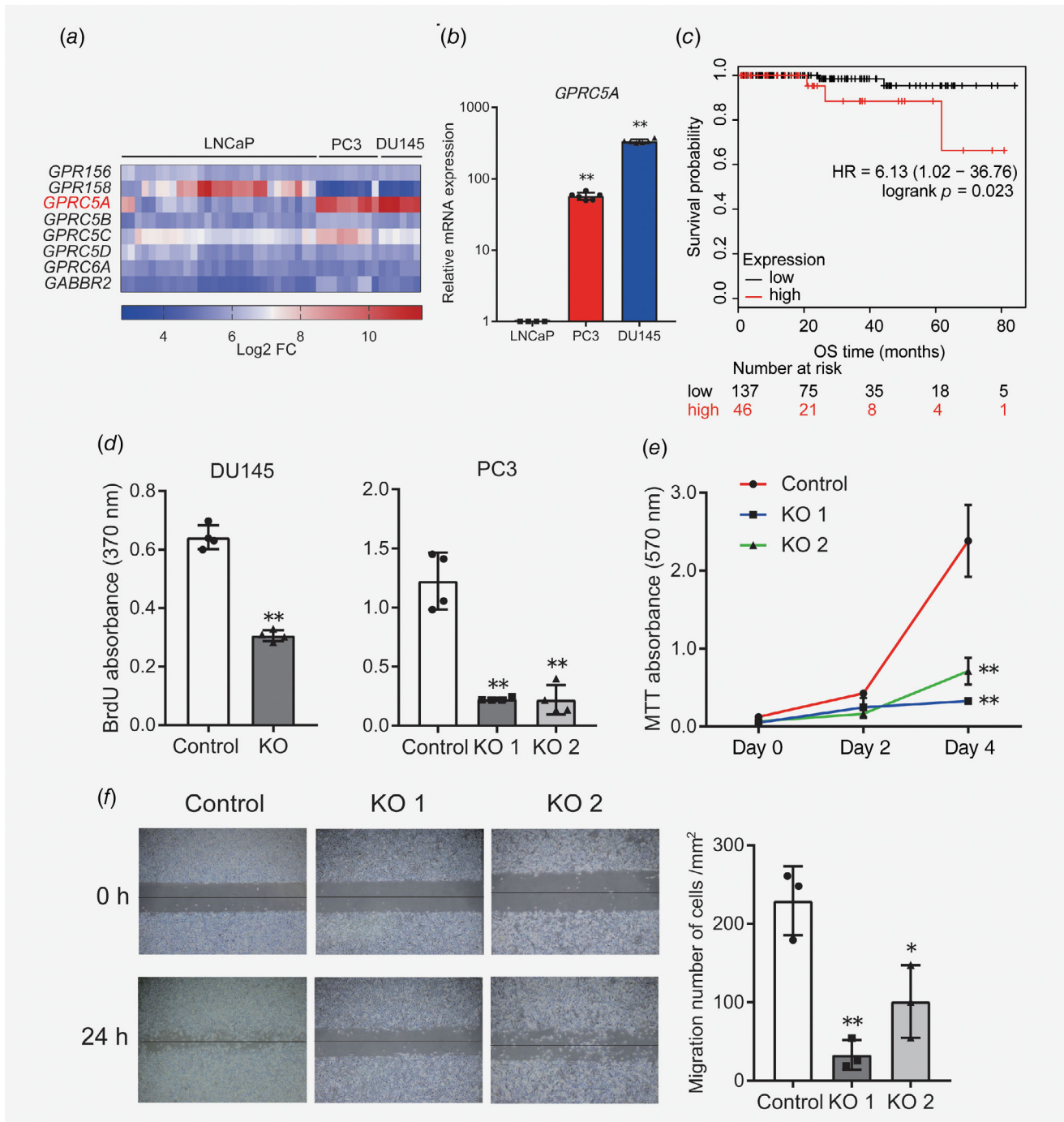


Figure 1. GPCR5A expression in prostate cancer cell lines, correlation to prognosis and cell proliferation. (a) Heat map of orphan GPCR class C family gene expression in PC3 and DU145 cells relative to LNCaP cells in a microarray data analysis (LNCaP: $n = 29$, PC3: $n = 9$, DU145: $n = 6$). (b) GPCR5A mRNA expression levels of LNCaP, PC3 and DU145 cells ($n = 3$). Data are presented as mean \pm SD. ** indicates $p < 0.01$ relative to LNCaP. (c) Kaplan–Meier curve showing correlation between high GPCR5A expression level and worse overall survival in prostate cancer patients. (d) Cell proliferation measured by ELISA BrdU incorporation in Control and GPCR5A KO DU145 and PC3 cells ($n = 4$). (e) Cell viability measured by MTT assay in Control and GPCR5A KO PC3 cells ($n = 3$). Cells were seeded at 1×10^4 cells/well in a 96-well plate and cultured for 2 and 4 days in a medium containing 7% FBS. (f) Cell migration activity measured by scratch assay in Control and GPCR5A KO PC3 cells ($n = 3$). Cells were seeded in six-well plates at 100% confluence, starved for 24 hr and scratched before measurement of cell migration 24 hr later. Data are presented as mean \pm SD. * and ** indicate $p < 0.05$ and $p < 0.01$, respectively, relative to Control.

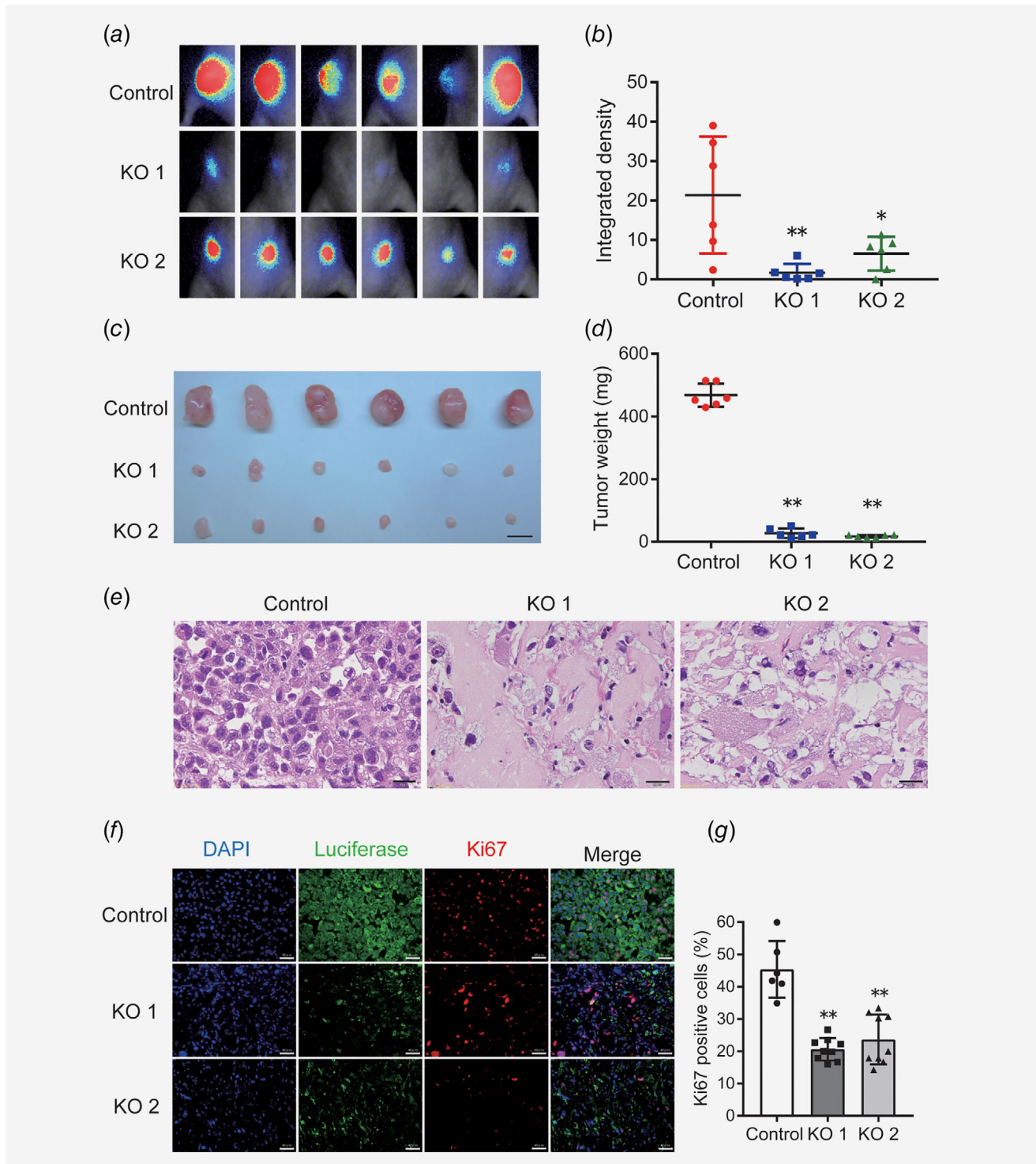


Figure 2. GPRC5A KO inhibited prostate cancer cell proliferation *in vivo*. (a) *In vivo* imaging of subcutaneous xenograft mice model. Control and GPRC5A KO PC3-Luc cells were inoculated at 0.75×10^5 cells/50 μ l in high-concentrate Matrigel. Five weeks after inoculation, luciferase was intraperitoneally administered and visualized ($n = 6$). (b) Quantitation of luminescence of subcutaneous tumors 5 weeks after inoculation. Quantitation was done by measuring the integrated grayscale density with ImageJ ($n = 6$). (c) Appearance of excised subcutaneous tumors (each group $n = 6$). Scale bar indicates 10 mm. (d) Weight of subcutaneous tumors at 5 weeks (each group $n = 6$). (e) Representative HE staining of subcutaneous tumor at 5 weeks. Bars indicate 20 μ m. (f) Representative immunohistochemistry for Luciferase (green), Ki67 (Red) and DAPI (blue) of tumor samples. Bars indicate 40 μ m. (g) Population of Ki67-positive cells among luciferase-positive cells in subcutaneous tumor sections (each group $n = 3$). Data are presented as mean \pm SD. ** indicates $p < 0.01$ relative to Control.

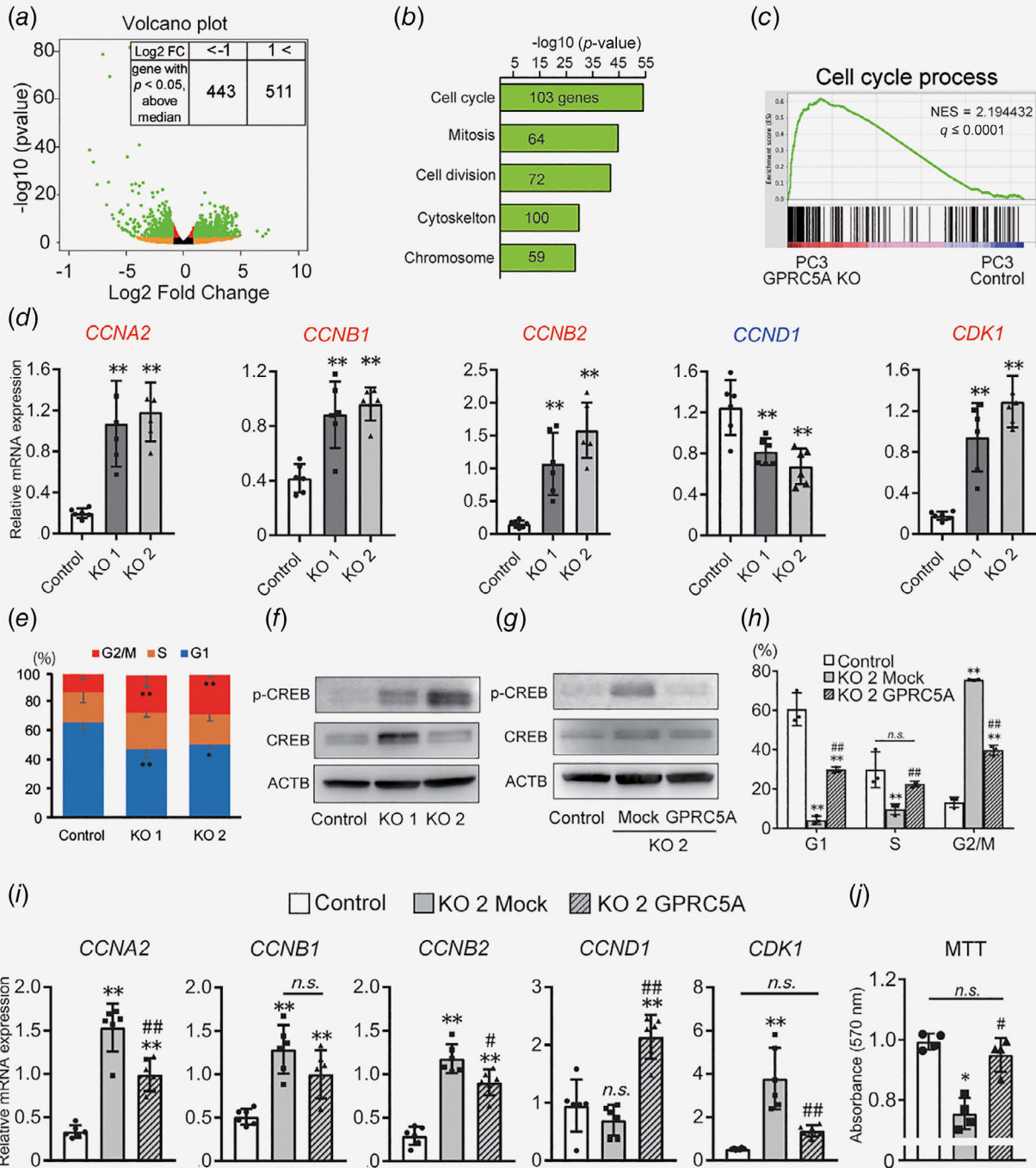


Figure 3. GPRC5A regulates the expression of cell cycle-related genes through CREB phosphorylation. (a) Volcano plot for RNA-seq data obtained from Control vs. GPRC5A KO PC3 cells (Control: $n = 3$, KO: $n = 6$). Green dots indicate genes that were significantly ($p < 0.05$) and differentially expressed in KO groups by more than twofold or were $<50\%$ of the Control. The number of differentially expressed genes is summarized in the table (inset). (b) Gene Ontology (GO) analysis using DAVID Bioinformatics Resources. The top five enriched biological processes by p -value together with gene counts are shown in the GO annotation chart. (c) GSEA plots for Cell cycle process-related genes that were significantly enriched in GPRC5A KO cells. (d) Real-time RT-PCR results for the expression levels of cell cycle-related genes ($n = 3$). Data are presented as mean \pm SD. * and ** indicate $p < 0.05$ and $p < 0.01$, respectively, relative to Control. (e) Flow cytometry of cell cycle status in Control and GPRC5A KO PC3 cells ($n = 5$). Data are presented as mean \pm SD. * and ** indicate $p < 0.05$ and $p < 0.01$, respectively, relative to Control. (f) Western blot for CREB and phosphorylated CREB in Control and GPRC5A KO PC3 cells. (g) Western blot for CREB and phosphorylated CREB in Control, Mock and GPRC5A overexpression GPRC5A KO 2 cells. (h) Percentage of each phase of cell cycle by flow cytometry in Control, Mock and GPRC5A overexpression GPRC5A KO 2 cells ($n = 3$). Data are presented as mean \pm SD. ** and ## indicate $p < 0.01$, relative to Control and Mock, respectively. (i) Real-time RT-PCR results for the expression levels of cell cycle-related genes in Control, Mock and GPRC5A overexpression GPRC5A KO 2 cells ($n = 3$). ** indicates $p < 0.01$, relative to Control. # and ## indicate $p < 0.05$ and $p < 0.01$, respectively, relative to Mock. *n.s.* indicates not significant. (j) Cell proliferation measured by MTT absorbance at day2 in Control, Mock and GPRC5A overexpression GPRC5A KO 2 cells ($n = 4$). * and # indicate $p < 0.05$, relative to Control and Mock, respectively. [Color figure can be viewed at [wileyonlinelibrary.com](https://onlinelibrary.wiley.com)]

These data indicate that GPRC5A KO cells might be arrested in the G2/M phase (Supporting Information Fig. S5b). To compare the expression levels of cell cycle-related genes between lung cancer and prostate cancer, we analyzed mRNA data of human lung and prostate cancers from the TCGA. The expression levels of cell cycle-related genes other than CCND1 are tended to be decreased in prostate cancer than lung cancer (Supporting Information Fig. S5c). Flow cytometry experiments to determine whether GPRC5A KO indeed affected cell cycle progression in prostate cancer cells exhibited that the proportion of cells in G2/M in both GPRC5A KO cell lines was significantly increased compared to control cells. Consistent with this result, the proportion of cells in the G1 phase was decreased in both PC3 and DU145 GPRC5A KO cells. (Fig. 3e and Supporting Information Fig. S5d). These results suggest that GPRC5A KO cells were arrested in the G2/M phase due to dysregulated expression of genes related to the cell cycle that subsequently led to decreased cell proliferation.

GPRC5A suppresses cAMP response element binding protein phosphorylation and positively regulates cell proliferation

GPCRs interact with G proteins that regulate the activity of adenylate cyclase and intracellular cyclic adenosine monophosphate (cAMP) concentration, which in turn affects protein kinase A (PKA) activation. Currently, there are no reports of G protein subtypes that couple with GPRC5A. Therefore, to understand how GPRC5A regulates intracellular signaling we examined phosphorylation levels of the cAMP response element binding protein (p-CREB) transcription factor. Western blotting showed that CREB phosphorylation levels were significantly increased in GPRC5A KO PC3 cells (Fig. 3f and Supporting Information Fig. S6a). CREB phosphorylation can also be induced by treatment of PC3-Luc cells with forskolin (Supporting Information Fig. S6b and S6c). Therefore, we used a BrdU incorporation assay to examine whether forskolin treatment affected PC3 cell proliferation. Treatment with either 30 or 60 μ M forskolin slightly but significantly reduced the amount of BrdU incorporation by PC3 cells (Supporting Information Fig. S6d). Next, we tried GPRC5A overexpression in GPRC5A knockout cells and successful overexpression of GPRC5A was confirmed in KO 2 cells (Supporting Information Fig. S6e). By GPRC5A overexpression, enhanced CREB phosphorylation in GPRC5A KO PC3 cells was decreased into the same level of control PC3 cells (Fig. 3g) and the cell cycle arrest at the G2/M phase was released (Fig. 3h) with partially rescued expression levels of cell cycle-related genes (Fig. 3h), followed by significant increased cell proliferation (Fig. 3j). These observations suggest that GPRC5A can inhibit CREB phosphorylation, which in turn enhances cell proliferation in progressive prostate cancer cells.

GPRC5A enhances establishment of prostate cancer bone metastasis

Patients with progressive prostate cancer and/or CRPC frequently have bone metastasis and poor prognosis. Zhou *et al.* reported that GPRC5A related to establishment of metastasis in

pancreatic cancer,²⁰ however, there is no report on the relationship between GPRC5A expression and prostate cancer metastasis. We tested if GPRC5A expression is correlated with bone metastasis and/or cancer growth. We examined GPRC5A expression levels in an expression data set for primary lesions from prostate cancer patients with or without bone metastasis²⁵ (GSE 6811, bone metastasis: $n = 3$, no bone metastasis: $n = 10$) that were obtained from the Oncomine gene expression database (<https://www.oncomine.org>). This data set showed that GPRC5A expression levels were significantly elevated in the primary lesions of prostate cancer patients with bone metastasis relative to those without metastasis (Fig. 4a), suggesting that GPRC5A may also be involved in the establishment of prostate cancer bone metastases. To further explore the role of GPRC5A in prostate cancer bone metastasis, we inoculated control PC3-Luc cells or GPRC5A KO PC3-Luc cells into the left tibial medullary space of nude mice. Tumor cell engraftment and size increases were confirmed weekly using *in vivo* bioluminescence imaging beginning 3 weeks after inoculation. Tumors arising from inoculated control PC3-Luc cells that had increased integrated density were apparent in *in vivo* imaging and beginning at 4 weeks after inoculation until euthanasia. In contrast, no luciferase signals could be detected in mice inoculated with GPRC5A KO PC3-Luc cells (Fig. 4b). By 6 weeks after inoculation, all mice in the control PC3-Luc cell group showed strong luminescence, whereas the group given GPRC5A KO PC3-Luc did not (Fig. 4c). These data support a critical role for GPRC5A in the establishment of bone metastasis as well as prostate cancer cell proliferation.

Furthermore, micro-CT analysis showed remarkable bone destruction in the proximal tibia of mice inoculated with control PC3-Luc cells. In contrast, the bone morphology in the GPRC5A knockout groups was the same as the intact group (Fig. 4d). The bone mineral density (BMD) of the proximal tibia in control group mice was also significantly lower than that of the intact group, but the GPRC5A KO group had similar density to that of the intact group (Fig. 4e). In histological evaluations by HE staining, prostate cancer cells were present in the intramedullary spaces of bone marrow from the control group, but not that of the GPRC5A KO group (Fig. 4f). TRAP staining, which specifically stains bone-resorbing osteoclasts, showed that the number of osteoclasts was increased on the surface of the bone matrix adjacent to tumor cells in the control group but not the GPRC5A KO groups (red staining, Fig. 4g), suggesting that inhibition of GPRC5A activity in progressive prostate cancer could ameliorate bone metastasis-induced bone destruction.

GPRC5A is frequently expressed in high-grade prostate cancer and correlates with the occurrence of bone metastases

To evaluate the clinical relevance of GPRC5A oncogenic synergy, we used immunohistochemistry to conduct GPRC5A expression analyses on 255 paraffin-embedded human prostate tumor samples that were collected from patients who

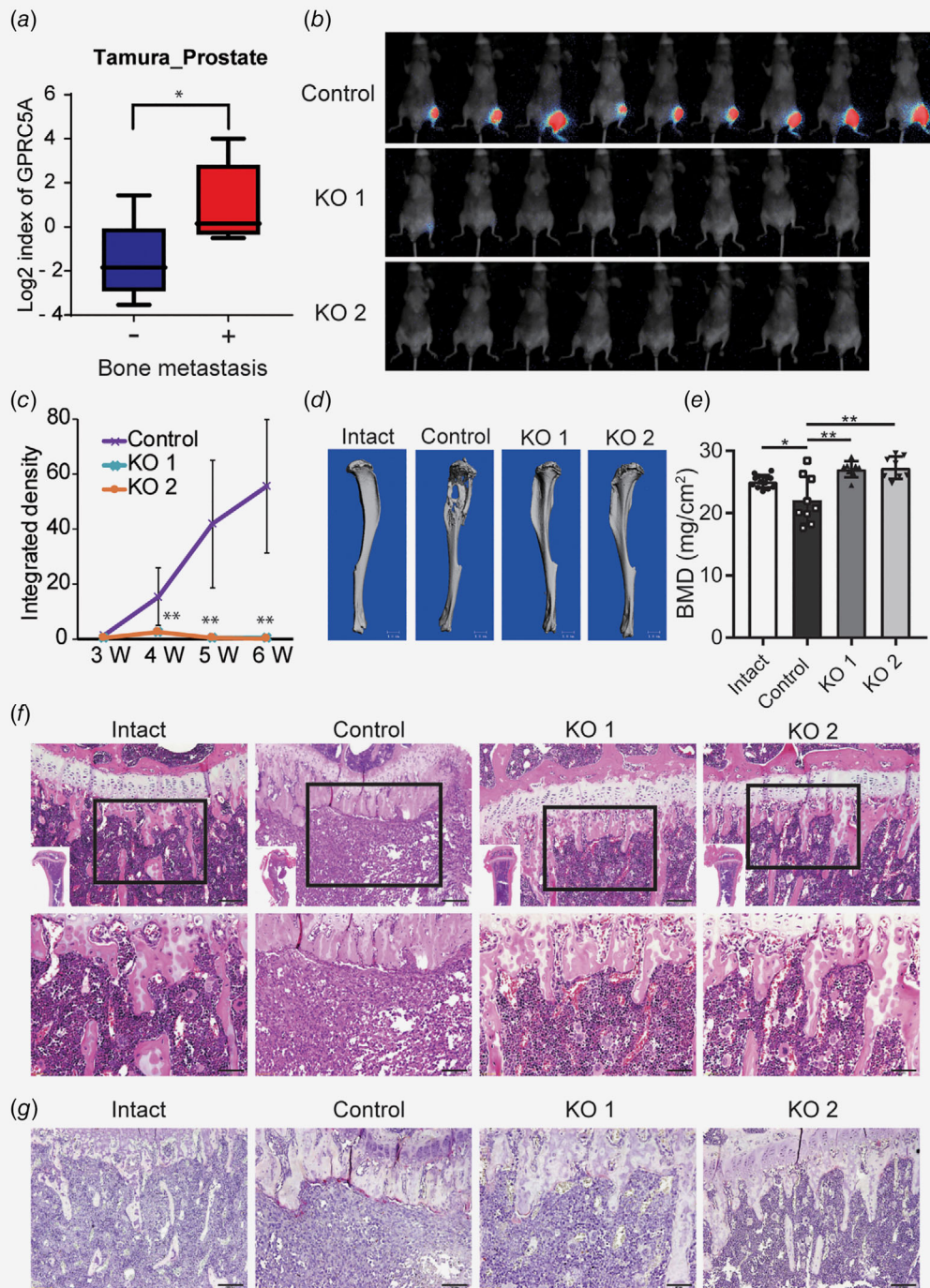


Figure 4. GPCR5A regulates establishment of prostate cancer bone metastasis. (a) GPCR5A expression levels in primary lesions of prostate cancer patients with no metastasis or bone metastasis in the registered microarray data as analyzed by GEO2R (Tamura *et al.*, GSE 6811, no metastasis: $n = 10$, bone metastasis: $n = 3$). Data are presented as mean \pm SD. * indicates $p < 0.05$ between two groups. (b) *In vivo* imaging of mouse tibial xenografts 6 weeks after inoculation. (c) Cells were transplanted into the left tibia at 1×10^4 cells/ $10 \mu\text{l}$ in PBS and luciferin was administered intraperitoneally every week beginning 3 weeks after transplantation. Quantitation was done by measuring the integrated grayscale density with ImageJ (Control: $n = 9$, KO 1: $n = 8$, KO 2: $n = 8$). Data are presented as mean \pm SD. ** indicates $p < 0.01$ relative to Control. (d) Micro-CT views of intact tibia and tibiae inoculated with Control and GPCR5A KO PC3 cells. Bars indicate 1 mm. (e) Bone mineral density of proximal 1/3 tibia (Intact: $n = 13$, Control: $n = 9$, KO1: $n = 8$, KO2: $n = 8$). Data are presented as mean \pm SD. * and ** indicate $p < 0.05$ and $p < 0.01$, respectively, relative to Control. (f) HE staining of proximal tibia. Bottom panels are higher magnification of boxed area in the respective top panel. Bars indicate 100 and 50 μm in the top and bottom panels, respectively. (g) TRAP staining of proximal tibia. Bars indicate 100 μm .

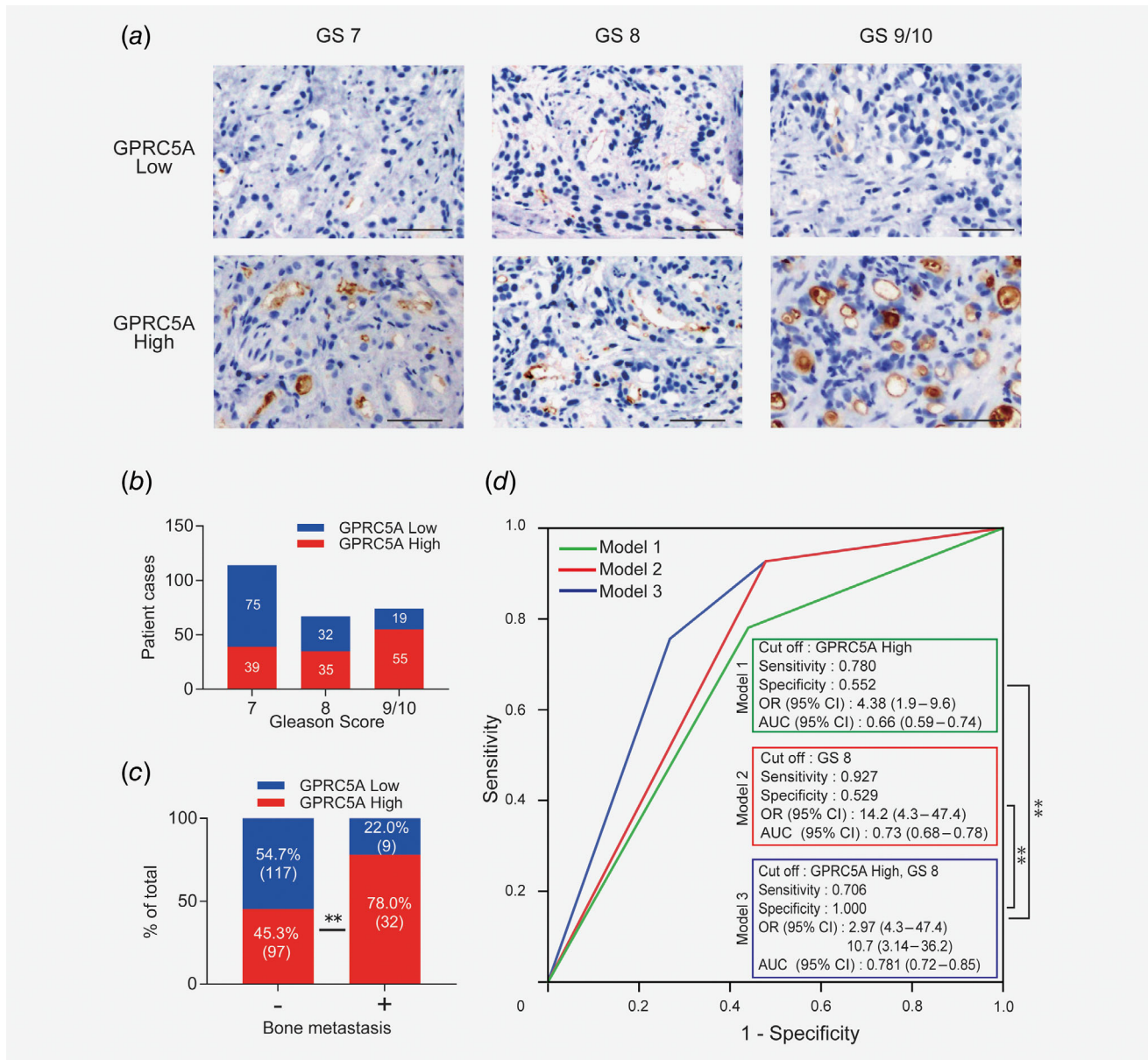


Figure 5. GPRC5A expression is correlated with malignancy and bone metastasis of prostate cancer in clinical samples. (a) Representative immunohistochemical staining of low/high immunoreactivity against GPRC5A on sections taken from formalin-fixed, paraffin-embedded GS7, 8 and 9/10 human prostate cancer specimens. Bars indicate 50 μm . (b) Assessment of GPRC5A immunoreactivity in 255 human prostate cancers categorized according to Gleason Score. (c) Percentage of GPRC5A immunoreactivity in 255 human prostate cancers categorized according to the presence or absence of bone metastasis (see Supporting Information Table S4). ** indicates $p < 0.01$ by Chi-squared test. (d) Results of logistic regression analysis and receiver operating characteristic (ROC) analysis on the occurrence of bone metastasis. ROC curves of the risk score for prostate cancer bone metastasis compared to GPRC5A immunoreactivity and/or Gleason Score (GS). The occurrence of bone metastasis was determined as the objective variable, and the GPRC5A immunoreactivity by IHC and GS were determined as explanatory variables. Abbreviations: OR, odds ratio; AUC, area under the receiver-operating characteristic curve; CI, confidence interval. ** indicates $p < 0.01$.

underwent transrectal prostate biopsy at the Division of Urology, Kanagawa Cancer Center. These patients had a Gleason's score (GS) of ≥ 7 and were evaluated for bone metastasis at the time of diagnosis. We analyzed the correlation between GPRC5A expression kinetics and the grade of prostate cancer as well as the onset of bone metastases. GPRC5A showed a

differential staining intensity and proportion that could be used to classify the samples into a Low or High immunoreactivity group according to the proportion of staining (Fig. 5a). The ratio of GS7 patients with high immunoreactivity was low (34.2%), whereas that for patients who were above GS8 was high (63.8%; Fig. 5b). In addition, patients with bone

Table 1. Bivariate analysis of GPCR5A immunoreactivity in human prostate cancer samples

Factor	<i>r</i>	<i>p</i>
Age	-0.071	0.253
Gleason Score	0.397 ¹	<0.01
Bone metastasis	0.238 ¹	<0.01

Correlation between GPCR5A immunoreactivity and age, Gleason Score (7–10) and the presence of bone metastasis for 255 prostate cancer patients. ¹*p* < 0.01.

metastasis had significantly higher GPCR5A immunoreactivity relative to patients without bone metastasis (78% vs. 45%; Fig. 5c and Supporting Information Table S4). A bivariate analysis showed a significant positive correlation between GPCR5A immunoreactivity, GS and bone metastasis (Table 1). To investigate whether analysis of GPCR5A expression could be useful for predicting the likelihood of bone metastasis, logistic regression analysis and receiver operating characteristic (ROC) analyses were performed using bone metastasis as a dependent variable, and GPCR5A immunoreactivity and GS as independent variables. The results demonstrated that GPCR5A immunoreactivity could indeed be a predictive marker of bone metastasis (OR: 4.38, *p* < 0.01, AUC: 0.666; Fig. 5d). Furthermore, by combining GPCR5A immunoreactivity and GS, the AUC was increased and the prediction accuracy was significantly improved with high specificity (AUC: 0.781; Fig. 5d). These results indicate that GPCR5A expression levels were correlated not only with prostate cancer aggressiveness but also with bone metastasis.

Discussion

Mechanisms underlying the progression and proliferation of prostate cancer are mainly based on AR activity. However, alternative pathway(s) outside of AR signaling are also associated with prostate cancer. Recently, various signaling pathways, such as growth factors, cytokines, miRNA and epigenetic control, were reported to be related to progression of prostate cancer and conversion into CRPC, indicating that these signaling pathways could be novel therapeutic targets.^{3,34,35} Among these alternate pathways, in our study, we focused on orphan GPCRs. Integrative analyses of gene expression profiles of prostate cancer cell lines indicated that expression levels of the orphan GPCR, GPCR5A, are significantly related to overall survival of prostate cancer patients, suggesting that GPCR5A can be a candidate therapeutic target molecule involved in prostate cancer progression (Fig. 1). It has been reported that GPCR5A knockdown reduces cell proliferation and migration ability in pancreatic cancer cell line.²⁰ As well as the previous report, we found that GPCR5A knockout remarkably decreased proliferation and migrating ability of progressive prostate cancer cell lines (PC3 and DU145) *in vitro* and *in vivo* (Figs. 1 and 2). This effect was associated with dysregulated expression of genes related to the cell cycle due to altered cAMP-CREB signaling (Fig. 3). Two

different types of GO analyses revealed that in the presence of GPCR5A KO, expression of genes involved in cell cycle processes was upregulated. Normal cell cycle progression is maintained by cyclic gene expression and protein degradation of cell cycle-related genes, such as CCNs and CDKs. Increased expression of cell cycle-related genes, particularly in specific cell cycle phases such as G2 and M, might lead to disorganized cyclic gene expression and protein degradation in GPCR5A KO cells. This disorganization in turn decreases rates of GPCR5A KO cell proliferation. These changes in gene expression profiles in GPCR5A KO cells were likely due to modifications in GPCR-dependent signal transduction. The cAMP-dependent pathway is a representative GPCR signaling cascade wherein cAMP plays an important role in intracellular signal transduction for activation of PKA that promotes phosphorylation of the transcription factor CREB.^{36,37} Although a G protein coupled to GPCR5A has not been reported, our results showing that CREB phosphorylation is enhanced by GPCR5A knockout indicate that GPCR5A could in fact be coupled with an inhibitory G protein (G α i). CREB can regulate transcription of various other transcription factors as well as genes that regulate metabolism, the cell cycle and secretion.³⁷ Therefore, dysfunction of the cAMP-dependent pathway can contribute to tumor development, tumor progression and also development of anticancer drug resistance.^{38,39} GPCR5A is known to contain a binding site for CREB in the 5' promoter region. Therefore, GPCR5A may form a negative feedback loop in which the phosphorylation of CREB is suppressed.¹⁹ The small molecule forskolin can promote CREB phosphorylation.⁴⁰ Here, both forskolin treatment and GPCR5A KO suppressed proliferation of prostate cancer cells (Fig. 3), suggesting that the cAMP-dependent pathway has negative regulatory effects on prostate cancer cell proliferation. However, the precise molecular mechanisms remain elusive. Regarding on the cell cycle regulation by GPCR5A in cancer cells, Deng *et al.* reported that GPCR5A negatively regulated CCND1 through NF- κ B signal in lung epithelial cells and suppressed cell proliferation and tumorigenesis.⁴¹ On the other hand, in our study, we showed that GPCR5A negatively regulated CREB phosphorylation, positively regulated CCND1 expression, and followed by increased cell proliferation of prostate cancer cells. This discrepancy might be partially explained by cell type specificity because the comparison of the expression of CCNA2, CCNB1, CCNB2, CCND1 and CDK1 mRNA between human lung cancer and prostate cancer samples by TCGA RNA-seq data (Supporting Information Fig. S5c.) showed different expression levels of cell cycle-related genes among cancer cell types. Therefore, more detailed study is needed to explore the mechanisms underlying GPCR5A mediated prostate cancer cell proliferation.

Bone metastasis and skeletal-related events (SREs) are one of the most crucial incidents for prostate cancer patients.⁴² Here we used a mouse intratibial xenograft model to demonstrate that GPCR5A also has a significant role in the establishment of bone metastasis (Fig. 4). Although GPCR5A KO cells exhibited

decreased cell proliferation, the effects of GPRC 5A KO were more obvious in the bone metastasis model (Fig. 4) relative to the subcutaneous inoculation model (Fig. 2). In addition, our clinical data indicated that GPRC5A expression levels were significantly correlated with bone metastasis (Fig. 5 and Table 1). The *in vitro* studies, such as invasion and adhesion analyses, could not support the involvement of GPRC5A in promoting prostate cancer bone metastasis, however, the *in vivo* and clinical studies support it. Therefore, to clarify the role of GPRC5A in bone metastasis, the elucidation of detailed molecular mechanism must be needed. Nonetheless, our results demonstrate that immunohistochemical analysis of GPRC5A levels could be a useful tool to diagnose prostate cancer patients who are likely to experience bone metastasis and thus require additional monitoring.

Our study has some limitations. We used only an osteolytic bone metastasis model with the PC3 cell line. However, bone metastasis in human prostate cancer is often mediated by osteoblasts through various mechanisms,^{43–45} whereas some prostate cancers exhibit osteolytic or mixed type bone metastasis.⁴⁶ As such, elucidation of the effects of GPRC5A in an osteoblastic bone metastasis model should be performed in a future study. In addition, our clinical study was cross-sectional and a longitudinal study on the relationship between GPRC5A and the occurrence of bone metastasis is needed.

Together with our results suggest that GPRC5A could be a therapeutic target for prostate cancer. On the other hand, GPRC5A is reported to act as a tumor suppressor in development of lung cancer.⁴⁷ In particular, GPRC5A expression on

the endoplasmic reticulum (ER) that mediates EGFR signaling in the ER is reported to dominate during development and progression of lung cancer.²² Thus, investigation of antagonistic antibodies against GPRC5A expressed on the plasma membrane would be needed to avoid possible side effects. Also, early diagnosis and early treatment for bone metastasis is vital for the prevention of SREs and treatment of established bone metastasis lesions with bisphosphonates or denosumab.⁴⁸

In summary, integrative analyses of registered data for prostate cancer identified GPRC5A as the most highly expressed gene among orphan GPCRs. GPRC5A KO suppressed prostate cancer proliferation and bone metastasis in a mouse model. Moreover, GPRC5A expression levels were significantly correlated with the occurrence of bone metastasis as well as prostate cancer progression. Our findings indicate that GPRC5A could be a novel therapeutic target molecule for progressive prostate cancer and a prognostic marker of bone metastasis.

Acknowledgements

The authors thank Dr. Naohito Tokunaga, the staff of the Division of Analytical Bio-Medicine and the Division of Laboratory Animal Research, the Advanced Research Support Center (ADRES), Ms. Aya Tamai and Ms. Sayoko Nakanishi and the members of the Division of Integrative Pathophysiology, Proteo-Science Center (PROS), Ehime University for their technical assistance and helpful support. Our study was supported in part by the Japan Society for the Promotion of Science (JSPS) KAKENHI Grants JP18K09168 (to TS, KT and YI) and JP16H06277 (Platform of Supporting Cohort Study and Biospecimen Analysis) and the Takeda Science Foundation.

References

- Norgaard M, Jensen AO, Jacobsen JB, et al. Skeletal related events, bone metastasis and survival of prostate cancer: a population based cohort study in Denmark (1999 to 2007). *J Urol* 2010;184:162–7.
- Denmeade SR, Isaacs JT. A history of prostate cancer treatment. *Nat Rev Cancer* 2002;2:389–96.
- Saraon P, Jarvi K, Diamandis EP. Molecular alterations during progression of prostate cancer to androgen independence. *Clin Chem* 2011;57:1366–75.
- Hussain M, Fizazi K, Saad F, et al. Enzalutamide in Men with nonmetastatic, castration-resistant prostate cancer. *N Engl J Med* 2018;378:2465–74.
- Alyamani M, Enamekhoo H, Park S, et al. HSD3B1(1245A>C) variant regulates dueling abiraterone metabolite effects in prostate cancer. *J Clin Invest* 2018;128:3333–40.
- Antonarakis ES, Lu C, Wang H, et al. AR-V7 and resistance to enzalutamide and abiraterone in prostate cancer. *N Engl J Med* 2014;371:1028–38.
- Day KC, Lorenzatti Hiles G, Kozminsky M, et al. HER2 and EGFR overexpression support metastatic progression of prostate cancer to bone. *Cancer Res* 2017;77:74–85.
- Culig Z, Hobisch A, Cronauer MV, et al. Androgen receptor activation in prostatic tumor cell lines by insulin-like growth factor-I, keratinocyte growth factor, and epidermal growth factor. *Cancer Res* 1994;54:5474–8.
- Malinowska K, Neuwirt H, Cavarretta IT, et al. Interleukin-6 stimulation of growth of prostate cancer in vitro and in vivo through activation of the androgen receptor. *Endocr Relat Cancer* 2009;16:155–69.
- Brauner-Osborne H, Wellendorph P, Jensen AA. Structure, pharmacology and therapeutic prospects of family C G-protein coupled receptors. *Curr Drug Targets* 2007;8:169–84.
- Tang XL, Wang Y, Li DL, et al. Orphan G protein-coupled receptors (GPCRs): biological functions and potential drug targets. *Acta Pharmacol Sin* 2012;33:363–71.
- Yang Y, Bai Y, He Y, et al. PTEN loss promotes intratumoral androgen synthesis and tumor microenvironment remodeling via aberrant activation of RUNX2 in castration-resistant prostate cancer. *Clin Cancer Res* 2018;24:834–46.
- Zhou C, Dai X, Chen Y, et al. G protein-coupled receptor GPR160 is associated with apoptosis and cell cycle arrest of prostate cancer cells. *Oncotarget* 2016;7:12823–39.
- Hobisch A, Culig Z, Radmayr C, et al. Androgen receptor status of lymph node metastases from prostate cancer. *Prostate* 1996;28:129–35.
- Bulanova DR, Akimov YA, Rokka A, et al. Orphan G protein-coupled receptor GPRC5A modulates integrin beta1-mediated epithelial cell adhesion. *Cell Adh Migr* 2017;11:434–46.
- Cheng Y, Lotan R. Molecular cloning and characterization of a novel retinoic acid-inducible gene that encodes a putative G protein-coupled receptor. *J Biol Chem* 1998;273:35008–15.
- Hofmann WK, de Vos S, Komor M, et al. Characterization of gene expression of CD34+ cells from normal and myelodysplastic bone marrow. *Blood* 2002;100:3553–60.
- Sokolenko AP, Bulanova DR, Iyevleva AG, et al. High prevalence of GPRC5A germline mutations in BRCA1-mutant breast cancer patients. *Int J Cancer* 2014;134:2352–8.
- Zhou H, Rigoutsos I. The emerging roles of GPRC5A in diseases. *Oncoscience* 2014;1:765–76.
- Zhou H, Telonis AG, Jing Y, et al. GPRC5A is a potential oncogene in pancreatic ductal adenocarcinoma cells that is upregulated by gemcitabine with help from HuR. *Cell Death Dis* 2016;7:e2294.
- Jaworska D, Krol W, Szliszka E. Prostate cancer stem cells: research advances. *Int J Mol Sci* 2015;16:27433–49.
- Wang J, Farris AB, Xu K, et al. GPRC5A suppresses protein synthesis at the endoplasmic reticulum to prevent radiation-induced lung tumorigenesis. *Nat Commun* 2016;7:11795.
- Zhong S, Yin H, Liao Y, et al. Lung tumor suppressor GPRC5A binds EGFR and restrains its effector signaling. *Cancer Res* 2015;75:1801–14.
- Irizarry RA, Hobbs B, Collin F, et al. Exploration, normalization, and summaries of high density oligonucleotide array probe level data. *Biostatistics* 2003;4:249–64.
- Tamura K, Furihata M, Tsunoda T, et al. Molecular features of hormone-refractory prostate cancer

- cells by genome-wide gene expression profiles. *Cancer Res* 2007;67:5117–25.
26. Labun K, Montague TG, Gagnon JA, et al. CHOPCHOP v2: a web tool for the next generation of CRISPR genome engineering. *Nucleic Acids Res* 2016;44:W272–6.
 27. Montague TG, Cruz JM, Gagnon JA, et al. CHOP-CHOP: a CRISPR/Cas9 and TALEN web tool for genome editing. *Nucleic Acids Res* 2014;42:W401–7.
 28. Yamashita M, Inoue K, Saeki N, et al. Uhrf1 is indispensable for normal limb growth by regulating chondrocyte differentiation through specific gene expression. *Development* 2018;145:dev157412.
 29. Epstein JI, Allsbrook WC Jr, Amin MB, et al. The 2005 International Society of Urological Pathology (ISUP) consensus conference on Gleason grading of prostatic carcinoma. *Am J Surg Pathol* 2005;29:1228–42.
 30. Huang d W, Sherman BT, Lempicki RA. Systematic and integrative analysis of large gene lists using DAVID bioinformatics resources. *Nat Protoc* 2009;4:44–57.
 31. Subramanian A, Tamayo P, Mootha VK, et al. Gene set enrichment analysis: a knowledge-based approach for interpreting genome-wide expression profiles. *Proc Natl Acad Sci USA* 2005;102:15545–50.
 32. Kanda Y. Investigation of the freely available easy-to-use software 'EZR' for medical statistics. *Bone Marrow Transplant* 2013; 48:452–8.
 33. Metz CE. Basic principles of ROC analysis. *Semin Nucl Med* 1978;8:283–98.
 34. Mishra R, Haldar S, Placencio V, et al. Stromal epigenetic alterations drive metabolic and neuroendocrine prostate cancer reprogramming. *J Clin Invest* 2018;128:4472–84.
 35. Xu K, Wu ZJ, Groner AC, et al. EZH2 oncogenic activity in castration-resistant prostate cancer cells is Polycomb-independent. *Science* 2012;338:1465–9.
 36. Goodman RH, Smolik S. CBP/p300 in cell growth, transformation, and development. *Genes Dev* 2000;14:1553–77.
 37. Zhang X, Odom DT, Koo SH, et al. Genome-wide analysis of cAMP-response element binding protein occupancy, phosphorylation, and target gene activation in human tissues. *Proc Natl Acad Sci USA* 2005;102:4459–64.
 38. Liu B, Yang H, Pilarsky C, et al. The effect of GPRC5a on the proliferation, migration ability, chemotherapy resistance, and phosphorylation of GSK-3beta in pancreatic cancer. *Int J Mol Sci* 2018;19:E1870.
 39. Gong S, Chen Y, Meng F, et al. Roflumilast enhances cisplatin-sensitivity and reverses cisplatin-resistance of ovarian cancer cells via cAMP/PKA/CREB-FtMt signalling axis. *Cell Prolif* 2018;51:e12474.
 40. Illiano M, Conte M, Sapio L, et al. Forskolin sensitizes human acute myeloid leukemia cells to H3K27me2/3 Demethylases GSKJ4 inhibitor via protein kinase a. *Front Pharmacol* 2018;9:792.
 41. Deng J, Fujimoto J, Ye XF, et al. Knockout of the tumor suppressor gene Gprc5a in mice leads to NF-kappaB activation in airway epithelium and promotes lung inflammation and tumorigenesis. *Cancer Prev Res (Phila)* 2010;3:424–37.
 42. Sartor O, de Bono JS. Metastatic Prostate Cancer. *N Engl J Med* 2018;378:645–57.
 43. Hashimoto K, Ochi H, Sunamura S, et al. Cancer-secreted hsa-miR-940 induces an osteoblastic phenotype in the bone metastatic microenvironment via targeting ARHGAP1 and FAM134A. *Proc Natl Acad Sci USA* 2018;115:2204–9.
 44. Li ZG, Mathew P, Yang J, et al. Androgen receptor-negative human prostate cancer cells induce osteogenesis in mice through FGF9-mediated mechanisms. *J Clin Invest* 2008; 118:2697–710.
 45. Schuettel LG, Link DC. Niche competition and cancer metastasis to bone. *J Clin Invest* 2011;121:1253–5.
 46. Lynch CC, Hikosaka A, Acuff HB, et al. MMP-7 promotes prostate cancer-induced osteolysis via the solubilization of RANKL. *Cancer Cell* 2005;7: 485–96.
 47. Jin E, Wang W, Fang M, et al. Lung cancer suppressor gene GPRC5A mediates p53 activity in nonsmall cell lung cancer cells in vitro. *Mol Med Rep* 2017;16:6382–8.
 48. Saad F, Sternberg CN, Mulders PFA, et al. The role of bisphosphonates or denosumab in light of the availability of new therapies for prostate cancer. *Cancer Treat Rev* 2018;68:25–37.